

Role of the range of the interactions in thermal conduction

Carlos Olivares¹ and Celia Anteneodo^{1,2}

¹*Department of Physics, PUC-Rio, Rio de Janeiro, Brazil*

²*Institute of Science and Technology for Complex Systems, Rio de Janeiro, Brazil*

(Dated: March 26, 2022)

We investigate thermal transport along a one-dimensional lattice of classical inertial rotators, with attractive couplings which decrease with distance as $r^{-\alpha}$ ($\alpha \geq 0$), subject at its ends to Brownian heat reservoirs at different temperatures with average value T . By means of numerical integration of the equations of motion, we show the effects of the range of the interactions in the temperature profile and energy transport, and determine the domain of validity of Fourier's law in this context. We find that Fourier's law, as signaled by a finite κ in the thermodynamic limit, holds only for sufficiently short range interactions, with $\alpha > \alpha_c(T)$. For $\alpha < \alpha_c(T)$, a kind of insulator behavior emerges at any T .

PACS numbers: 44.10.+i, 05.60.-k, 05.70.Ln, 66.30.Xj

I. INTRODUCTION

Heat conduction is a hot topic in non-equilibrium physics [1–13]. While there is a large body of works contributing to understand the empirically observed Fourier's law of conduction, many issues are still challenging, specially in low dimensions (see [14–16] and references therein). For one-dimensional systems, Fourier's law takes the form $J = -\kappa dT/dx$, where J is the flux, dT/dx the temperature gradient, and κ the heat conductivity, that depends on the system and can also depend on the temperature but not on system size. While, for systems with momentum non-conservative thermal noise [17, 18], an-harmonic pinned systems [19], or systems with local reservoirs [20], normal transport (hence, finite κ) is observed. Differently, anomalous transport typically occurs in other one-dimensional model systems [3, 21–27]. In those cases, the conductivity can exhibit a divergent dependence on system size and super-diffusion occurs [28], hence the Fourier's law is not satisfied. This scenario has been attributed to momentum conservation [25]. In apparent contradiction, the Fourier's law does hold for the momentum conservative model of rotators with nearest-neighbors interactions [29–35]. But, in this case, another quantity, the stretch, is not conserved [36]. However, when extra mechanical forces act at the extremities [37], counter-intuitive effects on the flux and on the temperature profile occur also in the rotators model.

Besides that, it is known that the range of the interactions can bring new features to a system. Ensemble inequivalence, phase transitions, relaxation times that increase with systems size and formation of quasi-stationary states, amongst others, can emerge when the interactions are sufficiently long-range [38–52]. In the present context, for instance, the long relaxation times observed in long-range systems [38, 45, 47] might affect thermal conductivity. Then, a natural question is: which is the influence of the range of the interactions in heat conduction? Addressing this issue, which can bring new insights to the above scenario, is the aim of the

present work. For that purpose, we consider a paradigmatic model system governed by a Hamiltonian dynamics, which generalizes the rotators model. It is known in the literature as α -XY [39, 40, 53], whose parameter α allows to adjust the range of the interactions from the nearest-neighbors to the global (mean-field) cases.

II. THE SYSTEM

The model α -XY consists of a chain of classical rotators, attached to the sites $i = 1, \dots, N$ of a one-dimensional lattice, whose dynamics is governed by the Hamiltonian [39, 40]

$$\begin{aligned} \mathcal{H}^\alpha &= \sum_{i=1}^N \frac{L_i^2}{2I_i} + \frac{\epsilon}{2} \frac{1}{\tilde{N}^\alpha} \sum_{i=1}^N \sum_{j \neq i}^N \left[\frac{1 - \cos(\theta_i - \theta_j)}{r_{i,j}^\alpha} \right] \\ &\equiv \sum_{i=1}^N \mathcal{H}_i^\alpha \equiv \sum_{i=1}^N [\mathcal{T}_i + \mathcal{U}_i^\alpha], \end{aligned} \quad (1)$$

where L_i is the angular momentum, I_i the rotational inertia, θ_i the angular position of the classical rotor, and we set

$$\tilde{N}^\alpha = \frac{1}{N} \sum_i \tilde{N}_i^\alpha, \quad \tilde{N}_i^\alpha = \sum_{j \neq i}^N r_{i,j}^{-\alpha}, \quad r_{i,j} = |i - j|, \quad (2)$$

in order to get a proper Kac prescription factor [54], that guarantees extensive energies in the thermodynamic limit (TL) when $\alpha \leq 1$ and is adequate to our (free) boundary conditions. In the limits $\alpha = 0$ and $\alpha \rightarrow \infty$, we recover the *infinite range* or mean-field (m-f) and *first nearest neighbors* (n-n) cases, respectively.

At the two ends of the lattice we apply (short-range) heat baths with temperatures T_L, T_R , with $T_L > T_R$. To model each reservoir, we use a Langevin heat bath.

Therefore, the equations of motion are

$$\begin{aligned}\dot{\theta}_k &= \omega_k, & \text{for } k = 1, 2, \dots, N, \\ I_k \dot{\omega}_k &= F_k^\alpha, & \text{for } k = 2, 3, \dots, N-1, \\ I_1 \dot{\omega}_1 &= F_1^\alpha - \gamma_L \omega_1 + \eta_L, \\ I_N \dot{\omega}_N &= F_N^\alpha - \gamma_R \omega_N + \eta_R,\end{aligned}\quad (3)$$

where ω_i is the angular velocity,

$$F_l^\alpha = -\frac{\partial \mathcal{H}^\alpha}{\partial \theta_l} = \sum_{k \neq l}^N f_{l,k}^\alpha, \quad f_{l,k}^\alpha = \frac{\epsilon}{N^\alpha} \frac{\sin(\theta_k - \theta_l)}{r_{k,l}^\alpha}, \quad (4)$$

$\gamma_{L/R}$ are the damping coefficients of the Langevin force and $\eta_{L/R}$ are white noises with correlations

$$\begin{aligned}\langle \eta_{L/R}(t) \eta_{L/R}(t + \tau) \rangle &= 2\gamma_{L/R} T_{L/R} \delta(\tau), \\ \langle \eta_L(t) \eta_R(t + \tau) \rangle &= 0.\end{aligned}\quad (5)$$

The flux is defined through the energy continuity equation for each particle, $\frac{d}{dt} \mathcal{H}_i^\alpha = \sum_{k \neq i}^N J_{i,k}^\alpha$, and, under the condition of local stationarity, we obtain the flow of heat towards the particle l due to the particle k

$$J_{l,k}^\alpha = \frac{1}{2} f_{l,k}^\alpha (\omega_k + \omega_l). \quad (6)$$

Hence, we define the flux from the left (right) particles towards the particle l as

$$\mathcal{J}_l^{L,\alpha} \equiv \left\langle \sum_{k < l}^N J_{l,k}^\alpha \right\rangle, \quad \mathcal{J}_l^{R,\alpha} \equiv \left\langle \sum_{k > l}^N J_{l,k}^\alpha \right\rangle. \quad (7)$$

In the stationary state $\mathcal{J}_l^{L,\alpha} = -\mathcal{J}_l^{R,\alpha}$, for all l . Moreover, the “temperature” at each particle position is defined as twice the mean kinetic energy $T_i = \langle I_i \omega_i^2 \rangle$, which allows to depict a temperature profile along the system length.

III. RESULTS

The equations of motion (3) were integrated by means of a Brownian dynamics protocol [55, 56] that reduces to a velocity-Verlet algorithm in the absence of interactions with the heat reservoirs, as in the case of the bulk particles, which are not directly coupled to the reservoirs. The fixed time step dt for numerical integration was selected so as to keep the energy of the corresponding isolated system constant within an error $\Delta E/E$ of order 10^{-4} . Initial conditions ($t = 0$) were set as follows: angles and momenta were randomly chosen around zero (and the average momentum subtracted), within intervals adequate to reproduce the equilibrium temperature $T \equiv (T_L + T_R)/2$ for the isolated system, before switching on the reservoirs. After the thermal baths are connected and a transient has elapsed, the quantities of interest were averaged over at least 30 different initial conditions

and along a time interval $\Delta t = 10^6$. Without loss of generality, in the numerical simulations reported here, we fixed the following values of the parameters of the Hamiltonian (1): $\epsilon = 2$, $I_i = 1.0$ for all i , and $\gamma_L = \gamma_R = 1.0$.

In Fig. 1, we show typical temperature profiles for different values of α . These profiles for $T = 0.8$ and $\Delta T = 0.2$ do not change substantially for values of N larger than the value used in the Fig. 1. We observe that, in the bulk region, the profiles are almost linear. The absolute value of the slope is very close to its maximal value ΔT for n-n interactions ($\alpha \rightarrow \infty$), but the curves become less steep as α decreases. For sufficiently long-range interactions, when $\alpha < \alpha_c \simeq 1$, the bulk profile becomes flat, and also more noisy.

The stationary flux \mathcal{J}^α through the chain was computed by averaging Eq. (7) over the bulk particles, namely, $\mathcal{J}^\alpha \equiv \langle \mathcal{J}_l^\alpha \rangle_{bulk}$. The scaled flux $N\mathcal{J}^\alpha$, for fixed α , is depicted as a function of the size N in Fig. 2, for the same values of the end temperatures considered in Fig. 1. For α above α_c , the scaled flux grows with N attaining a finite value, like in the n-n limit [29–31]. Differently, for any α below α_c , the scaled flux monotonically decays with N . Therefore, a distinct behavior of $N\mathcal{J}^\alpha$ vs N emerges for short and long range interactions. In the limit case $\alpha = 0$, the scaled flux presents a neat decay as $1/N$, indicating that the flux vanishes in the TL. Apparently, a decay towards zero flux also occurs for any $\alpha < \alpha_c$. It is noteworthy that, although the temperature profiles for small α are very similar to those observed for chains of identical masses with n-n harmonic interactions [27], differently, in the latter case the flux is significantly non null.

Let us analyze the m-f case ($\alpha = 0$). In the TL, a null current along the chain is expected, because, on the one hand, each rotor interacts with each other rotor with equal intensity, on the other, the contribution of the end

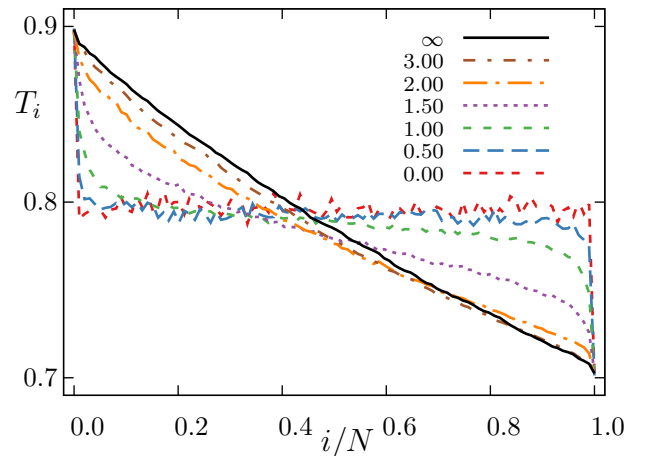


FIG. 1. Temperature profiles for different values of α indicated on the figure. For each α , averages over 50 realizations are computed. $T \equiv (T_L + T_R)/2 = 0.8$, $\Delta T \equiv T_L - T_R = 0.2$, and $N = 100$.

rotors (which are the only ones able to break the m-f symmetry) becomes negligible compared to the interaction with the bulk. Therefore, the lattice structure where rotors are attached is superfluous and there is not a preferential direction for the flux. From another viewpoint, it is as if the two reservoirs were placed anywhere. Even if the current through the chain decays in the TL, there is a flow of energy from the hot to the cold reservoir. In fact, the end rotors are directly coupled to the heat reservoirs and, as a consequence, there is a current from the hot bath to the first rotor, which is the same current from the last rotor to the cold reservoir. This current is split in several paths: one is the short-circuit given by the long-range coupling between the two end particles and other paths go through each rotor i , that is, passing from the first particle through the bulk particle i towards the last one. But, noteworthy, a net current does not pass “through” the chain, then $N\mathcal{J}^\alpha = 0$. For a finite system, even if the bulk rotors still interact globally, a small current exists, because in that case the effect over each bulk rotor due to the end rotors is not negligible. Consistently with this view, the current $N\mathcal{J}^\alpha$ decays with N . This scenario which is clear for the m-f case ($\alpha = 0$), apparently also emerges for any α below α_c , while, of course, it breaks down for sufficiently short-range interactions.

Once the bulk flux due to given applied end temperatures is computed, the heat conductivity κ can be estimated through

$$\mathcal{J} \simeq \kappa \Delta T / N, \quad (8)$$

for small enough difference between the temperatures applied at the ends, ΔT . Therefore, the plots in Fig. 2 for $N\mathcal{J}^\alpha$ vs N (which were computed for fixed T_L and T_R), directly reflect the behavior of the thermal conductivity κ with N and α .

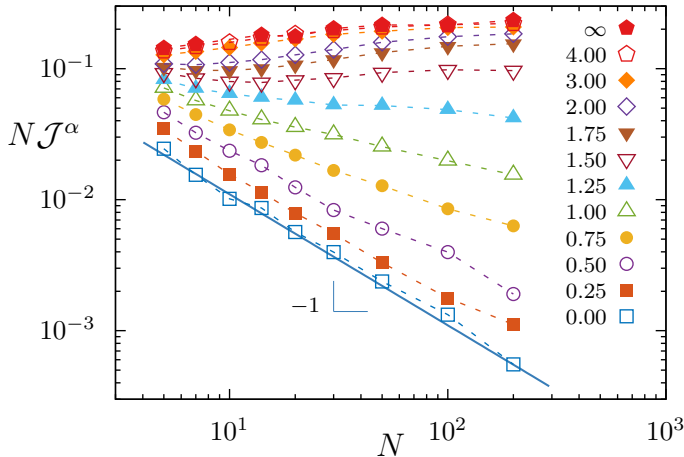


FIG. 2. Scaled flux $N\mathcal{J}$ vs N , for different values of α indicated on the figure. Dashed lines are guides to the eye. The relative standard error associated to each symbol is about 100%, 10% and 1% for $\alpha \in (0, 1)$, $(1, 2)$ and $(2, \infty)$, respectively. The solid line, with slope -1, was drawn for comparison. $T \equiv (T_L + T_R)/2 = 0.8$ and $\Delta T \equiv T_L - T_R = 0.2$.

We can observe in Fig. 2 that, for fixed size N , the scaled flux (hence κ), continuously increases with α . Therefore, short range interactions favor heat transport. Above $\alpha \simeq 3$, κ practically attains the level of the n-n dynamics for all N .

For fixed α , when the range is short enough ($\alpha > \alpha_c$), we notice that κ tends to a finite value in the large size limit, indicating the validity of Fourier’s law. Differently, below α_c , κ decreases with N , apparently following a power-law decay $N^{-\beta}$, where $\beta \simeq 1$ for $\alpha = 0$, and the exponent β decreases with α , vanishing above α_c . This suggests that κ becomes null in the TL for systems with $\alpha < \alpha_c$. However, much larger sizes, which are computationally infeasible, would be required to determine the precise decay law.

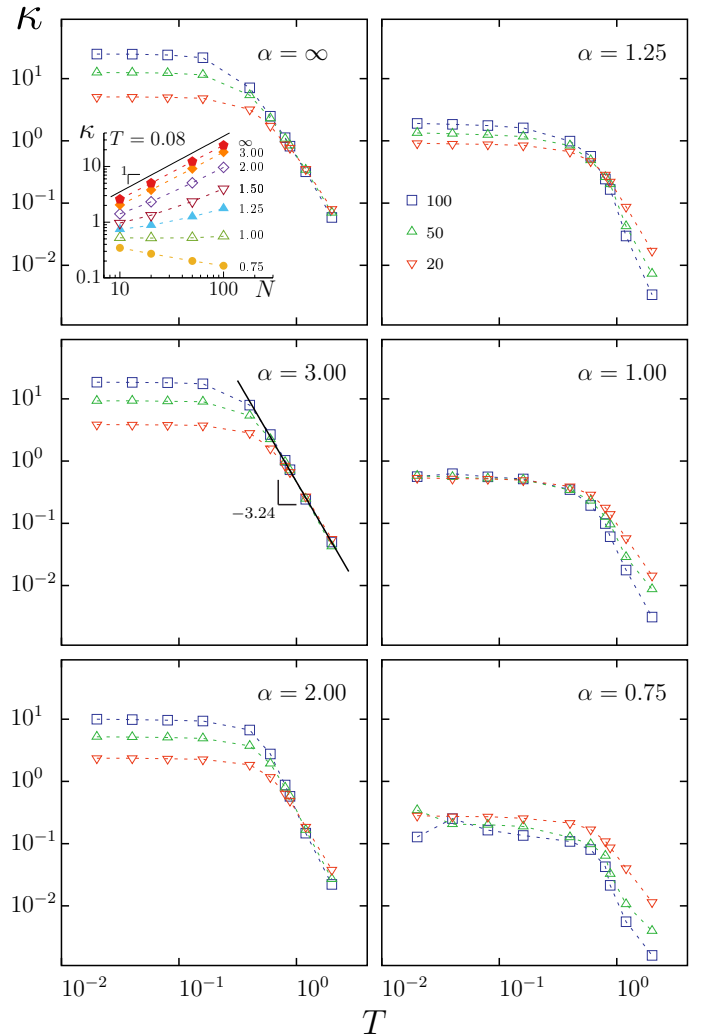


FIG. 3. Conductivity κ vs temperature T , for different system sizes and fixed α indicated on each panel. In case $\alpha = 3$, we show a power-law fit to the plots of $\kappa(T)$ in the high temperature range. In the inset, we show the dependency of κ with N at a low temperature ($T = 0.08$), for different values of α . In all cases, $\Delta T/T = 0.25$. Dotted lines are guides to the eye.

We also investigated the dependency of κ with the mean temperature T , as depicted in Fig. 3.

Let us comment first on the dependency of κ with T for fixed size N . For any α , we observe that, the heat conductivity does not depend on T at low temperatures, but there is a crossover to a high temperature regime where κ decays with T . In the limit of sufficiently low temperature, particles feel the nearly harmonic bottom of the potential well, reaching the limit of harmonic oscillators. At very high temperatures, a decay with T is expected, because, the kinetic energy becomes much larger than the potential one (which is bounded for the α -XY Hamiltonian), then, rotors tend to behave as independent particles, and, concomitantly, any transport process tends to become hindered.

Next we discuss the impact of α on the dependency of κ with N . Let us look at the three leftside panels of Fig. 3. The scenario for any $\alpha \geq 2$ is the same observed for n-n interactions ($\alpha \rightarrow \infty$). At low temperature, κ increases with N (see also the inset, for $T = 0.08$). The high temperature decay seems to follow a power-law, with the same exponent observed for n-n interactions (about -3.2 [29]), as illustrated for $\alpha = 3$ in Fig. 3. Furthermore, at high T , the curves for different sizes tend to coincide, consistently with our previous observation of a limiting value of κ in the large size limit, when we discussed Fig. 2 which was built for $T = 0.8$.

When the interactions are short-range ($\alpha > 1$), the level of the flat region of $\kappa(T)$, observed for low temperatures below the crossover, grows linearly with N (see inset in the upper left panel), as expected for a chain of harmonic oscillators. However, notice that, concomitantly with that increase of the flat level with N , the crossover temperature diminishes with N , suggesting that the curves $\kappa(T)$ for different values of N tend to adhere to a same curve as N increases (which occurs progressively at lower temperature and larger conductivity). If that were the case, the growth of κ with N would persist only at null temperature, but, at a given finite T , the conductivity would increase sublinearly with N stabilizing at a finite value in the TL. Then, Fourier's law would hold. This possibility is in accord with previous claims [29, 32, 34] against the divergence of the conductivity in the TL [30, 33, 35], for n-n interactions, but much higher sizes would be required to confirm the result for any $\alpha > 1$.

At the particular value $\alpha = 1$, we observe that the flat region of the conductivity profile coincides for different values of N (constant κ in inset plot), while for $\alpha < 1$ (illustrated by the case $\alpha = 0.75$), the conductivity decays with system size. This points that $\alpha = 1$ is a marginal case at low temperatures.

At very low temperatures, a particle feels an harmonic potential, regardless the value of α . However, in the case of long-range interactions, the harmonic approximation does not come solely from n-n interactions. Then the level of the flat region does not increase with N , but differently to the harmonic chain behavior, κ decreases

with N , becoming presumably vanishingly small in the TL.

Now consider the rightside panels of Fig. 3 (that is, $\alpha < 2$), as well as the inset plot. For temperatures above the crossover, a distinctive feature in comparison with the leftside panels appears: the conductivity decays with N , suggesting vanishingly small values in the TL (like in Fig. 2).

Therefore, for long-range interactions ($\alpha < 1$), κ decays with N for any T , in accord with our discussion for the m-f case where the conductivity vanishes in the limit $N \rightarrow \infty$ at any finite temperature.

The observed behavior of κ with N , for different values of T and α , is summarized in the diagram of Fig. 4. We indicate whether, for the studied range of N , κ vs N attains a finite value (F) or not, and in this latter case whether the behavior is decreasing (D) or increasing (I) with N . Much larger sizes would be required to determine the TL. This is limited by the computational cost, taking into account that the integration algorithm is of order N^2 , and stabilization times also increase with N . Moreover, deviations from the diagram shown in Fig. 4 may occur for a different ratio $\Delta T/T$, therefore this dependency should be also investigated, but again this is limited by the computational capacity.

Although one would expect a priori a threshold at $\alpha = d = 1$ (where $d = 1$ is the lattice dimensionality), the curve $\alpha_c(T)$ that emerges from simulations goes from

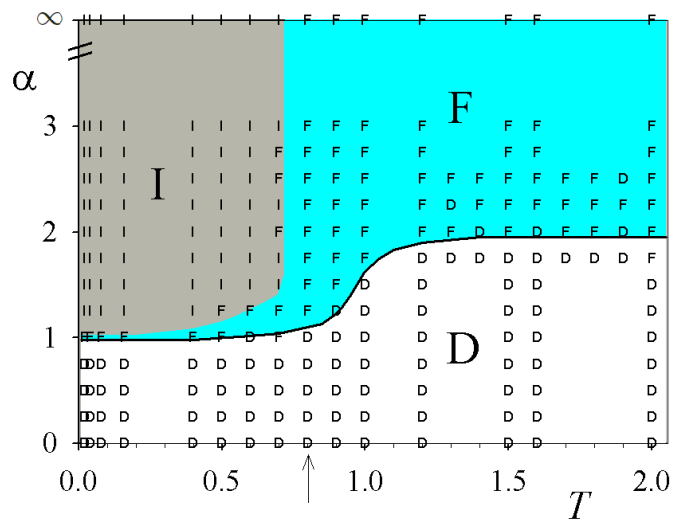


FIG. 4. Diagram in the plane $T - \alpha$ of the different thermal regimes of the conductivity κ : conductivity attains a finite value (F) or not, either decreasing (D) or increasing (I) with N , for the investigated range of N . From plots of $\kappa \sim N\mathcal{J}$ vs N , like in Fig. 2, we obtained the classification indicated by characters for each pair (T, α) , with $\Delta T/T = 0.25$. The arrow highlights the outcomes for $T = 0.8$, in agreement with the results shown in Fig. 2, although ΔT is slightly different. The black solid line represents the critical value $\alpha_c(T)$.

$\alpha_c \simeq 1$ at low temperatures to $\alpha_c \simeq 2$ at high temperatures. Also in this case, a distortion due to finite sizes can not be discarded. But, coincidentally, the change of regime occurs near the critical temperature ($T^* = 1$) at which the isolated system in equilibrium suffers a ferro-paramagnetic transition when $\alpha \leq 1$ (a transition also exists for $1 < \alpha < 2$, although at smaller T^*) [39].

IV. FINAL REMARKS

In summary, we have shown the portrait of heat conduction for a one-dimensional system of interacting particles as a function of the range of the interactions. The different domains are sketched in the diagram of Fig. 4. We conclude that, the longer the range of the interactions, more the thermal conduction is spoiled. An interesting finding is the occurrence of a kind of insulator behavior for $\alpha < \alpha_c(T)$ (white region, denoted by ‘D’, in the diagram of Fig. 4).

For $\alpha > \alpha_c$, the thermal behavior is analogous to that found for nearest neighbor interactions. That is, for high temperatures, the thermal conductivity stabilizes at a finite value (‘F’) in the large size limit, decaying with T following a power law. For low temperatures, the conductivity increases with N (‘I’). Although, for the studied sizes, we do not observe stabilization of κ at a finite

value, a picture similar to that observed for n-n interactions [29, 32, 34] emerges, pointing to the validity of Fourier’s law.

Differently, when interaction are sufficiently long-range ($0 \leq \alpha \leq \alpha_c$), the scaled flux $N\mathcal{J}^\alpha$ (hence the conductivity) decays with N for any T (‘D’), apparently vanishing in the TL, like is expected in the limiting mean-field case $\alpha = 0$. Then, the bulk system presents a flat temperature profile and it behaves like an insulator, in the sense that the flux through the chain is vanishingly small. This poor thermal conductivity is consistent with the slow relaxation to equilibrium observed in long-range systems, like in the Hamiltonian Mean-Field ($\alpha = 0$) [38, 45] or a modified Fermi-Pasta Ulam model [47], where collisional effects act over times that increase with N , differently to short-range systems. The impact on thermal conductivity of other recent results about perturbation propagation, where no finite group velocity limits the spreading of perturbations and supersonic propagation occurs [57] in long-range systems, also deserves investigation. Finally, note that it is plausible that the nontrivial scenario here reported for one-dimension can be extended to an arbitrary dimension d , for $\alpha \mapsto \alpha/d$, which might also deserve a future extension of this work.

Acknowledgments: We thank Brazilian agencies CNPq and Faperj for partial financial support.

-
- [1] S. Lepri, R. Livi, A. Politi in *Thermal Transport in Low Dimensions: From Statistical Physics to Nanoscale Heat Transfer* Chap. 1, S. Lepri, editor (Springer International Publishing, 2016).
 - [2] G. T. Landi, M. J. de Oliveira, *Phys. Rev. E* **87**, 052126 (2013).
 - [3] Y. Li, S. Liu, N. Li, P. Hänggi, B. Li, *New J. Phys.* **17**, 043064 (2015).
 - [4] L. Wang, L. Xu, H. Zhao, *Phys. Rev. E* **91**, 012110 (2015).
 - [5] S. G. Das, A. Dhar, K. Saito, C. B. Mendl, H. Spohn, *Phys. Rev. E* **90**, 012124 (2014).
 - [6] C. B. Mendl, H. Spohn, *Phys. Rev. E* **90**, 012147 (2014).
 - [7] A. V. Savin, Y. A. Kosevich, *Phys. Rev. E* **89**, 032102 (2014).
 - [8] Sha Liu, Junjie Liu, Peter Hänggi, Changqin Wu, Baowen Li, *Phys. Rev. B* **90**, 174304 (2014).
 - [9] D. Xiong, Y. Zhang, H. Zhao, *Phys. Rev. E* **90**, 022117 (2014).
 - [10] N. Yang, G. Zhang, B. Li, *Nano Today* **5**, 85 (2010).
 - [11] L. Wang, T. Wang, *Europhys. Lett.* **93**, 54002 (2011).
 - [12] L. Wang, B. Hu, B. Li, *Phys. Rev. E* **86**, 040101 (2012).
 - [13] N. Li, J. Ren, L. Wang, G. Zhang, P. Hänggi, B. Li, *Rev. Mod. Phys.* **84**, 1045 (2012).
 - [14] S. Lepri, R. Livi, A. Politi, *Phys. Rep.* **377**, 1 (2003).
 - [15] F. Bonetto, J. L. Lebowitz, L. Rey-Bellet, In *Math. Physics 2000*, chapter 8, pages 128–150. (Word Scientific, 2000).
 - [16] A. Dhar, *Adv. in Physics* **57**, 457 (2008).
 - [17] G. T. Landi, M. J. de Oliveira, *Phys. Rev. E* **89**, 022105 (2014).
 - [18] A. Dhar, K. Venkateshan, J. L. Lebowitz, *Phys. Rev. E* **83**, 021108 (2011).
 - [19] K. Aoki, D. Kusnezov, *Phys. Lett. A* **265**, 250 (2000).
 - [20] F. Bonetto, J. L. Lebowitz, J. Lukkarinen, *J. Stat. Phys.* **116** 783 (2004).
 - [21] S. Liu, P. Hänggi, N. Li, J. Ren, B. Li, *Phys. Rev. Lett.* **112**, 040601 (2014).
 - [22] B. Li, J. Wang, *Phys. Rev. Lett.* **91**, 044301 (2003).
 - [23] O. Narayan, S. Ramaswamy, *Phys. Rev. Lett.* **89**, 200601 (2002).
 - [24] K. Aoki, D. Kusnezov, *Phys. Rev. Lett.* **86**, 4029 (2001).
 - [25] T. Prosen, D. K. Campbell, *Phys. Rev. Lett.* **84**, 2857 (2000).
 - [26] H. Nakazawa, *Prog. Theor. Phys. Supplement* **45**, 231 (1970).
 - [27] Z. Rieder, J. L. Lebowitz, E. Lieb, *J. Math. Phys.* **8**, 1073 (1967).
 - [28] G. Basile, C. Bernardin, S. Olla, *Comm. in Math. Phys.* **287**, 67 (2009).
 - [29] Y. Li, N. Li, B. Li, *Eur. Phys. J. B* **88** 1 (2015).
 - [30] O. V. Gendelman and A. V. Savin, *Phys. Rev. Lett.* **84**, 2381 (2000).
 - [31] C. Giardinà, R. Livi, a. Politi, and M. Vassalli, *Phys. Rev. Lett.* **84**, 2144 (2000).
 - [32] L. Yang, B. Hu, *Phys. Rev. Lett.* **94**, 219404 (2005).
 - [33] O. V. Gendelman, A. V. Savin, *Phys. Rev. Lett.* **94**, 219405 (2005).
 - [34] L. Yang, P. Grassberger, arxiv.org/abs/cond-mat/0306173

- [35] E. Pereira, R. Falcao, *Phys. Rev. Lett.* **96**, 100601 (2006).
- [36] S. G. Das, A. Dhar, arxiv.org/pdf/1411.5247
- [37] A. Iacobucci, F. Legoll, S. Olla, G. Stoltz, *Phys. Rev. E* **84**, 1 (2011).
- [38] L. Moyano, C. Anteneodo, *Phys. Rev. E* **74**, 021118 (2006).
- [39] F. Tamarit, C. Anteneodo, *Phys. Rev. Lett.* **84**, 208 (2000).
- [40] C. Anteneodo, C. Tsallis, *Phys. Rev. Lett.* **80**, 5313 (1998).
- [41] M. Antoni, S. Ruffo, *Phys. Rev. E* **52**, 2361 (1995).
- [42] A. Campa, T. Dauxois, S. Ruffo, *Phys. Rep.* **480**, 57 (2009).
- [43] F. L. Antunes, F. P. C. Benetti, R. Pakter, Y. Levin, *Phys. Rev. E* **92**, 052123 (2015).
- [44] A. Campa, S. Gupta, S. Ruffo, *Journal of Statistical Mechanics: Theory and Experiment* **5**, P05011 (2015).
- [45] T. N. Teles, S. Gupta, P. Di Cintio, L. Casetti, *Phys. Rev. E* **92**, 020101 (2015).
- [46] S. Gupta, T. Dauxois, S. Ruffo, *Europhys. Lett.* **113**(6), 60008 (2016).
- [47] G. Miloshevich, J. Nguenang, T. Dauxois, R. Khomeriki, S. Ruffo, *Phys. Rev. E* **91**, 032927 (2015).
- [48] T. M. Rocha Filho, A. E. Santana, M. A. Amato, A. Figueiredo, *Phys. Rev. E* **90**, 032133 (2014).
- [49] Y. Levin, R. Pakter, F. B. Rizzato, T. N. Teles, F. P.C. Benetti, *Phys. Rep.* **535**(1), 1-60 (2014).
- [50] P. de Buyl, G. De Ninno, D. Fanelli, C. Nardini, A. Patelli, F. Piazza, Y. Y. Yamaguchi *Phys. Rev. E* **87**, 042110 (2013).
- [51] C. Nardini, S. Gupta, S. Ruffo, T. Dauxois, F. Bouchet, *J. Stat. Mech.* **01**, (2012) L01002.
- [52] S. Gupta, D. Mukamel, *Phys. Rev. Lett.* **105**, 040602 (2010).
- [53] C. Anteneodo, *Physica A* **342** 112 (2004).
- [54] M. Kac, G. E. Uhlenbeck, P. C. Hemmer, *J. Math. Phys.* **4**, 216 (1963).
- [55] M. G. Paterlini, D. M. Ferguson, *Chem. Phys.* **236**, 243 (1998).
- [56] M. P. Allen, D. J. Tildesley, *Computer Simulation of Liquids*. (Clarendon Press, 1987).
- [57] D. Métivier, R. Bachelard, M. Kastner, *Phys. Rev. Lett.* **112**, 210601 (2014).